Clim. Past Discuss., doi:10.5194/cp-2016-68, 2016
Manuscript under review for journal Clim. Past
Published: 27 July 2016
© Author(s) 2016. CC-BY 3.0 License.

Climate of the Past Discussions
Open Access
EGU

Deforestation decreases resistance of simulated Easter Island climate to drought

Alexander Lemburg[1,2], Martin Claussen[1,2], and Felix Ament[1,2]

[1]Max Planck Institute for Meteorology, Hamburg D-20146, Germany
[2]Meteorological Institute, University of Hamburg D-20146, Germany

Correspondence to: Alexander Lemburg (alexander.lemburg@mpimet.mpg.de)

Abstract. Easter Island underwent a rapid deforestation several hundred years ago. The causes have been discussed in depth. However, the effect of the deforestation on the near-surface climate of Easter Island and possible feedbacks have not yet been studied. Here we use the limited-area model COSMO to simulate a series of typical weather situations for a fully tree-covered, grass-covered and a bare soil Easter Island, respectively. We find that the top soil layer of the deforested island becomes much warmer and the wind speed roughly doubles, thereby enhancing the erosion on the deforested island. During a drought spell, evapotranspiration decreases much more slowly over a forested area. If the soil has become dry, then the tree-covered island triggers convective precipitation much more efficiently than the bare-soil or grass-covered island could do. This is caused by the higher surface roughness and stronger sensible heat flux which lead to a deeper boundary layer and an enhanced moisture flux convergence over the forested island. Hence, the climate of a deforested Easter Island appears to be significantly less resistant to drought than a forested island and thus, deforestation has probably exacerbated the effects of past climate drought spells on Easter Island socio-ecological systems.

1 Introduction

Easter Island, a small remote island (about 160km^2) in the south-eastern Pacific Ocean located about 3700km off the coast of Chile at 27.1° S and 109.3° W, is characterized by a warm and oceanic climate with roughly 1100 mm of precipitation per year and an annual mean temperature of 20.5 °C. Mean monthly rainfall shows some seasonality with the driest period in austral spring and summer and a maximum during austral autumn (see Supporting Information Text S1 for a detailed description of climate). The first humans, most likely Austronesian Polynesians, arrived on Easter Island sometime between 800 AD and 1300 AD (Martinsson-Wallin and Crockford, 2001; Hunt and Lipo, 2006; Wilmshurst et al., 2011).

Since the first discovery by Edward Davis in 1687 and Jacob Roggeveen in 1722, the island has attracted wide interest in many scientific disciplines because of its remarkable flora with mostly sparse grassland and barely any trees. Deforestation of Easter Island can be narrowed down to a time frame between 1200 and 1650 AD (Mann et al., 2003; Orliac, 2000; Mieth et al., 2002). Pollen data indicate that before that time and even during the last glacial, the island was covered by a dense palm forest (Flenley and King, 1984; Flenley et al., 1991; Bork and Mieth, 2003) with perhaps up to 16 million trees (Bork and Mieth,

Clim. Past Discuss., doi:10.5194/cp-2016-68, 2016
Manuscript under review for journal Clim. Past
Published: 27 July 2016
© Author(s) 2016. CC-BY 3.0 License.

2003). One of the dominant trees was a native palm species (*Paschalococos disperta*) that is related to the Chilean wine palm (*Jubaea Chilensis*) which is still found in parts of Chile (Martinsson-Wallin, 2004).

While many studies agree that the islanders were mainly responsible for the deforestation (Mieth and Bork, 2010; Mann et al., 2008; Flenley et al., 1991), climatic variations might have played a role in the deforestation process. Numerical simulations using a complex Earth system model (Junk and Claussen, 2011) do not reveal any strong changes in climate during the last millennium which could have led to forest decline. However, some studies suggest that Easter Island experienced a considerable phase of climatic deterioration characterized by prolonged droughts (Hunter-Anderson, 1998; Mc Call, 1994; Orliac and Orliac, 1998) during the Little Ice Age. Oxygen isotope depletion at Lake Rano Kao accompanied by the disappearance of tree pollen suggest a notable cool-dry climate event roughly 550 years ago within this period (Gossen, 2011).

Even if large-scale climate variability was not responsible for the deforestation, we assume that the replacement of the once dense woodland by sparse grassland could had influenced the island's local climate in a way that natural forest regrowth could had been severely limited. To explore the effect of the deforestation on near-surface climate and local rainfall, we use the limited area model COSMO (Doms and Baldauf, 2015) and perform numerical simulations of typical weather situations for three different land surface setups that portray a fully tree-covered island, a grass-covered island and an island covered only by typically dark bare soil (see Methods 2.1 and 2.2). To study potential effects of droughts, all simulations were repeated starting from low, medium and high soil moisture with 10%, 50% and 80% saturation with regard to the pore volume, respectively. Hence we assess the potential impact of past deforestation on the resistance of the Easter Island atmosphere – vegetation system to past and present drought spells.

2 Methods and Data

2.1 Numerical model

We use version 4.11 of the COSMO-CLM (Consortium for Small-Scale Modelling Model in Climate Mode) which is the climate version of the COSMO model (Rockel et al., 2008). The COSMO model, based on the former Lokal-Modell (LM) (Doms and Schättler, 1999), is a non-hydrostatic limited-area atmospheric prediction model (Doms and Baldauf, 2015) designed for operational weather forecast as well as for various scientific research applications on small and medium mesoscale phenomena. It is based on the primitive thermo-hydrodynamical equations describing compressible flow in a moist atmosphere. We run COSMO with its standard second generation land surface and soil model TERRA-ML (Schrodin and Heise, 2001) (more informations are available in Supporting Information Text S2).

For the investigation of the impact of the deforestation on the local climate, we need very high spatial resolution in our numerical model in order to have a reasonable amount of island grid points and to directly simulate small-scale phenomena as convection. We choose a resolution of 0.01° which corresponds to a grid point spacing of approximately 1.1 km (in the following, this will be called just 1 km). In order to realize such high-resolution simulations, a double one-way nesting is performed where we use 6-hourly ECMWF (European Centre for Medium-Range Weather Forecasts) analysis data at 0.25° resolution for a preceding 7 km simulation which output is then used as boundary and initial data for the final 1 km runs. The

Clim. Past Discuss., doi:10.5194/cp-2016-68, 2016
Manuscript under review for journal Clim. Past
Published: 27 July 2016
© Author(s) 2016. CC-BY 3.0 License.

model domain for the coarse and fine simulations and the model topography of the high-resolution run are illustrated in figure 1 (for more technical information, see Supporting Information Text S3).

2.2 Experiment strategy and analysis

We choose specific synoptic case studies as the very high resolution does not allow continuous simulation for longer time periods. Instead of typical one-day studies, we use three or four day-long synoptic case studies to allow sufficiently divergent developments for each run and to be able to deduce averages for specific times of day for each case study. To study the changes in energy fluxes and near-surface temperatures, we select 3 weather situations characterized by mostly clear skies and moderate wind. In the following, these clear sky case studies receive the acronym CSC(+number). 11 distinct rainfall events are used to examine the impacts on precipitation . Of those, 4 can be described as large-scale rain events (LSP) and 7 are characterized by convective activity (CP). A detailed description of the large-scale synoptic situations is given in Table S2 in the Supporting Information.

For every case study, three 1 km simulations will be run with a fixed set of land surface parameters (leaf area index, vegetation cover, surface albedo, roughness length) which portray a fully tree-covered island (TC), a complete bare soil island (BS), and a grass-covered island (GC) (see Supporting Information Text S4 and Table S1). To study potential effects of droughts, we also run each land surface simulation with different initial soil moisture settings, where we set each of the eight soil layers to an initial relative moisture of 80%, 50% and 10% with regard to soil pore volume.

By this method, we end up with a set of 9 main experiments for each case study as depicted in figure 2. In the following, those experiments may be referred to by an acronym that is composed of an abbreviation for the land surface and the initial soil moisture (example: BS-50, bare soil island with an initial soil moisture of 50%). Additionally to these main experiments we also perform a set of specific sensitivity simulations for three distinct precipitation cases in which we test how the local rainfall is affected by the presence of an island, its size and topography (Supporting information Text S6).

Precipitation, especially of convective origin, is a problematic quantity due to its complex formation mechanism, high spatial inhomogeneity and strong dependency on the initial state. Therefore, all simulations of the 11 precipitation case studies are conducted as a mini ensemble consisting of five members which are generated by the domain shifting method (Supporting Information Text S5).

For the interpretation of our results, we mostly consider the area average of the 156 Easter Island grid points in our model and neglect further investigation of spatial gradients within the island area. We compare primarily accumulated precipitation between each land surface setting for each initial soil moisture setting. Additionally to rainfall we also look at quantities as sensible heat flux or boundary layer moisture flux convergence averaged over the entire case study for specific times of day. The boundary moisture flux convergence is represented by the average convergence of all model layers below roughly 700 m. We give the results in form of bar plots as in Figure 1 where we indicate the standard deviation of the 5-member ensemble with error bars. Between each land surface setting, the student-t test is applied to check for the statistical significance in unclear cases.

Clim. Past Discuss., doi:10.5194/cp-2016-68, 2016
Manuscript under review for journal Clim. Past
Published: 27 July 2016
© Author(s) 2016. CC-BY 3.0 License.

Climate of the Past Discussions
Open Access
EGU

2.3 Frequency of undisturbed convective weather situations

For the evaluation of our result's relevance, we analyse the frequency of synoptically undisturbed convective weather situations in the Easter Island region. We assume that such situations are characterized by low synoptic wind speeds, the occurrence of some convective rain and the availability of Convective Available Potential Energy (CAPE). By means of a 35-year long (1979-2014) ERA-Interim reanalysis data set (Dee et al., 2011) at a spatial resolution of 0.125°, we apply a simple measure to estimate an upper limit for the frequency of such weather situations: For each day of the reanalysis data (13149 days), we look at a 6×6 array around Easter Island spanning from 27.375° S to 26.75° S and from 109.75° W to 109.125° W and find the spatial maximum (CAPE, convective precipitation) or minimum (wind speed) of the diurnal mean value. If this field maximum (minimum for wind) is above (below for wind) a certain value, it is assumed that the Easter Island region as a whole meets this condition. We choose 100 J/kg CAPE, 0.5 mm convective precipitation and 7.5 m/s 10 m wind speed as threshold values and count all days that fulfil these conditions simultaneously.

2.4 Soil drying experiment

To assess the speed of the soil drying process and the sustainability of humid surface and near-surface conditions characterized by high latent heat fluxes, we conduct a prolonged soil drying experiment for the tree-covered and bare soil island. For that, we choose a dry, high-insolation case study of 4 days and perform it 13 times. As a starting point, a soil moisture of 80% with regard to the pore volume is used. At the end of each case study, the soil moisture of the grid cell with the highest soil drying rate is used to provide the initial soil moisture for all island grid cells for the next simulation. Eventually, we receive an upper limit estimation for the soil drying over a period of 52 days.

2.5 Frequency of drought spells

We estimate the frequency of droughts by using daily precipitation records from Mataveri Airport (Direccion Meteorologica de Chile, 2016) in addition to ERA-Interim data. To guarantee a certain comparability, both data sets comprise the exact same time interval from January 1979 to December 2014, with 1990 missing. To get an upper limit estimation of the occurrence of dry periods, the ERA-Interim daily precipitation is always the field minimum of the Easter Island region. Following method is used to detect and count dry periods: Daily precipitation is accumulated for a certain amount of days in the range of 15 to 60 days. If the accumulated rain does not exceed a certain value (e.g. 5 or 10 mm), this time interval is counted as a dry period. The intervals have to be disjoint and separated by at least 10 days (3 days in case of 7-day dry periods) in order to be counted as two different dry periods.

Clim. Past Discuss., doi:10.5194/cp-2016-68, 2016
Manuscript under review for journal Clim. Past
Published: 27 July 2016
© Author(s) 2016. CC-BY 3.0 License.

3 Results

3.1 Impact on precipitation

At first, we conduct sensitivity experiments where we test the role of the island's size and topography on precipitation for distinct synoptic case studies. In weather situations with large-scale precipitation and convective precipitation with higher synoptic forcing (fronts, higher wind speeds), no significant differences in simulated area-averaged rainfall over Easter Island with different land-surface conditions can be detected. The amount of area-averaged precipitation over the adjacent ocean, over an Easter Island without orography, over an Island which has the same topography as Easter Island, but has a 10 times larger area, is mostly statistically indistinguishable (see Supporting Information Figs. S2,S3). The orography of Easter Island affects only the spatial distribution and the local intensity of rainfall.

For synoptically undisturbed convective situations, however, a clear imprint of the island on precipitation is found. Figure 3 shows the accumulated precipitation of four days with low synoptic forcing and weak wind speeds in December 2004. In the simulation with a normal-sized bare soil island (3a), some shower cells form at the north-eastern part of the island, likely due to coastal convergence. If we remove the island from the model domain, all rain showers vanish (3b). The topography of Easter Island has some minor effects but does not change the area-averaged rainfall significantly. Figure 3d and 3e show that the intensity and area-averaged amount of precipitation clearly scales with the size of the island. From these sensitivity tests it is evident that Easter Island is large enough to generate a mesoscale circulation which triggers local rainfall over the island in suitable conditions.

We use the same synoptic situation for our set of the nine main experiments concerning the impact of deforestation. In Figure 4, the area-averaged precipitation sum, forenoon sensible heat, afternoon moisture flux convergence and the spatial distribution of precipitation over Easter Island is depicted for different land-surface configurations and different initial soil moisture, representing different states of drought. Precipitating convection is triggered irrespective of initial soil moisture mainly on the north-eastern shore (Fig. 4d-f). When soil moisture is high, only small differences in rainfall are found between a forested and a deforested island. Interestingly, dry soils appear to trigger more precipitation and more intense rainfall than wet soils. Moreover, in dry soil conditions, differences between surface types become clearly visible. A forested island with dry soils attracts much more rain than a deforested, barren or grass-covered, island.

On average, the dry forested island shows a much higher sensible heat flux in the forenoon due to its high roughness (Fig. 4b). We argue that the strong sensible heating of the planetary boundary layer (PBL) promotes the strongest mesoscale sea-breeze circulation, characterized by the highest PBL moisture flux convergence (Fig. 4c). In combination with sufficiently unstably stratified PBL air, the tree-covered island therefore sees the highest convective activity. Additional variables for this particular case study are presented in Supporting Information Fig S4-S6. Three other case studies (Supporting Information Figs S7-S9), characterized by high instability and very low synoptic forcing as well, show a very similar behaviour. We always find that in cases of medium or high soil moisture, the deforestation does not lead to significant changes in precipitation. But with dry soils, the forested island always shows increased rainfall. Averaged over all four case studies (Table 1), precipitation over the bare soil Easter Island decreases by roughly 45 percent in comparison with the tree-covered island.

Clim. Past Discuss., doi:10.5194/cp-2016-68, 2016
Manuscript under review for journal Clim. Past
Published: 27 July 2016
© Author(s) 2016. CC-BY 3.0 License.

Climate of the Past Discussions

The increase in convective precipitation with decreasing soil moisture can be interpreted as a negative, dampening feedback. Drier soils lead to earlier and/or enhanced convective rainfall which, in turn, leads to higher soil moisture which will then weaken convective activity. This feedback is much stronger over a forested Easter Island. In addition, there is strong drought-buffering effect of forests. In the prolonged soil drying experiment (see Methods 2.4), we find that it takes at least one month of dry weather for the soil to dry such that the latent heat fluxes become considerably low on the tree-covered island (Figure 5a/c). The tree roots are able to steadily extract water from deeper soil layers until the wilting point (24% for the used soil type) is reached. For a deforested (bare soil) Easter Island, evapotranspiration ceases much faster (Figure 5b/d) because the moisture diffusion flux to the soil surface abates fast after approaching 50% soil moisture. This fast decline might be overestimated in TERRA-ML (see Supporting Information Text S2, last section).

3.2 Impact on near-surface climate

To study the effect of a complete deforestation on the near-surface climate of Easter Island, we analyse three simulations in which insolation is rather strong. Figure 6 shows the diurnal cycle of turbulent heat fluxes, temperatures and wind for three consecutive days of one particular simulation. This case represents three days in January 2011 which are characterized by high insolation and rather low wind speeds. Because of the small (prescribed) albedo differences between grass land, bare soil and forest cover, differences in net radiation play a minor role in the energy budget compared to the strongly different evapotranspiration potential of trees, grass and bare soil. The tree-covered island is able to sustain a constant high latent flux even if we initialize with 50% soil moisture for which, by contrast, the bare soil island does not show any latent flux any more. This is a consequence of the aforementioned limitation of bare soil evaporation by the moisture diffusion flux. Because grass has a rather shallow root depth and, in our model, a bare soil fraction of 30%, the simulations with a grass-covered island (dashed lines) also show a rapidly declining latent heat flux (Fig. 6b).

Whereas nighttime temperatures do not differ much, we see strongly increased daytime temperatures for the grass-covered and bare soil island. With high soil moisture, an initial midday air temperature difference between the tree- covered and the bare soil island grows from 1 K to roughly 2 K due to the quick reduction of evaporative cooling (Fig. 6c). On the soil surface, the differences are much more pronounced with differences up to 20 K (Fig. 6d). As the forested island has by far the highest surface roughness, the turbulent heat fluxes are generally considerably higher over the forested island than over the bare-soil or grass-covered island. This is especially visible in the case of dry soils where latent heat fluxes vanish. In this situation, the tree-covered island shows sensible heat fluxes up to nearly 800 W/m^2 whereas the other land surfaces with much lower roughness only reach about 600 W/m^2 (Fig. 6c). We also see a strong convergent sea-breeze circulation evolving due to the strong sensible heating (Fig. 6f). Additional variables are given in Supporting Information Table S3.

The above-mentioned soil drying experiment shows that after about six days, the initial soil moisture of 80% drops to about 50% in the uppermost soil layers on the bare soil land which nearly leads to a vanishing of bare soil evaporation whereas the tree-covered island keeps a relatively steady latent heat flux, even after some more days of dry weather. We think it is therefore reasonable to compare the area-averaged maximum air and surface temperatures between our tree-covered simulations at 80% and bare soil simulations at 50% soil moisture to assess the maximum impact of the deforestation on temperatures. Taking all

Clim. Past Discuss., doi:10.5194/cp-2016-68, 2016
Manuscript under review for journal Clim. Past
Published: 27 July 2016
© Author(s) 2016. CC-BY 3.0 License.

three different high-insolation cases into account, we find that the maximum gap in 2 m temperature amounts to 2.8 K and up to 22 K at the soil surface. The minimum of the near-surface relative humidity decreases by at least roughly 20 percentage points in every simulation. In addition to that, all case studies show roughly a doubling in average near-surface wind speeds (Table 2).

3.3 Climatological relevance

Since weather situations with low wind and convective conditions are critical for the occurrence of strong effects of deforestation, we try to assess the question of how often such conditions occur in present-day climate. We analyse time series from the ERA-Interim data base (Dee et al., 2011) and measurements from Mataveri Airport (Direccion Meteorologica de Chile, 2016). To give an upper limit estimate on the frequency of critical weather periods, we apply a simple analysis scheme (see Methods 2.3). We use CAPE, precipitation and near surface wind ERA-Interim data of the last 35 years and count those days during which the CAPE exceeds a diurnal mean of 100 J/kg, the precipitation exceeds 0.5 mm, and the wind stays below 7.5 m/s (see also Supporting Information Fig S12 and Table S4). We find that about 13.5% of all days satisfy this condition. These contribute to the total rain amount with a share of 27.5%. Hence as an upper limit, about one quarter of annual precipitation falls in undisturbed convective conditions which can potentially be impacted by varying surface conditions on Easter Island.

A second important question concerns the occurrence of dry periods on Easter Island. In the ERA-Interim data and the Mataveri Airport data, we find that significant dry periods with less than 10 mm of rain accumulation in 60 days have not been recorded in 35 years (1979 – 2014). 30-day periods with less than 10 mm precipitation occur roughly every two years according to measurement records and every 16 months if we use ERA-Interim as an estimate. The longest registered dry period with less than 10 mm lasted 48 and 38 days, respectively (see Supporting Information Table S5).

4 Conclusions

We have found that Easter Island shows a clear imprint on precipitation in undisturbed convective weather conditions. Soil moisture then plays a key role in determining the strength of convective activity. The comparison of different land surface setups showed that as long as the soil moisture is high or normal, the vegetation does not seem to significantly influence area-averaged precipitation. In cases of drought, however, the tree-covered island shows strongly increased convective precipitation. This is caused by the enhanced surface roughness and higher sensible heat flux which lead to a sufficiently deep boundary layer and an enhanced moisture flux convergence over the forested island.

Higher wind speed over the deforested Easter Island likely favours erosion. A second stressor of plant seedlings could be the strong warming of upper soil layers with maxima reaching 50 °C in our simulations, if a complete bare soil is considered. For most plant species, the onset of heat-induced tissue damage is between 50 – 55 °C (Kolb and Robberecht, 1996). Perhaps, enhanced seedling mortality could have accelerated the deforestation process by curbing regrowth. Another consequence of the high soil surface temperature is an increased water vapour deficit which can also be very harmful for tree seedlings (Will et al., 2013).

Clim. Past Discuss., doi:10.5194/cp-2016-68, 2016
Manuscript under review for journal Clim. Past
Published: 27 July 2016
© Author(s) 2016. CC-BY 3.0 License.

By a simple analysis of the last few decades we have shown that longer dry periods are most likely rare in modern day climate. Hence in present-day climate, the stabilizing atmosphere – forest interaction unfolds rarely. However in a climate with more frequent or more intense droughts, which could have happened over Easter Island in the past (Hunter-Anderson, 1998; Mc Call, 1994; Orliac and Orliac, 1998; Gossen, 2011), this interaction was presumably more important. Deforestation could have enhanced the severity of droughts by weakening the negative soil moisture - convective precipitation feedback. In combination with generally less humid near-surface conditions, stronger erosion and possibly increased seedling mortality, a large-scale deforestation over Easter Island during such climate period likely pushed the near-surface conditions in a mode unsustainable for forest regrowth.

Author contributions. A.L. and M.C designed the research and A.L carried out the simulations. All authors discussed the results and contributed to the manuscript.

Acknowledgements. The authors wish to thank Andrea Lammert-Stockschlaeder for providing the ECMWF analysis files used as forcing data for the COSMO simulations. Computational resources were made available by Deutsches Klimarechenzentrum (DKRZ) through support from Bundesministerium für Bildung und Forschung (BMBF).

Clim. Past Discuss., doi:10.5194/cp-2016-68, 2016
Manuscript under review for journal Clim. Past
Published: 27 July 2016
© Author(s) 2016. CC-BY 3.0 License.

Climate of the Past Discussions
Open Access
EGU

References

Bork, H.-R. and Mieth, A.: The key role of Jubaea palm trees in the history of Rapa Nui: a provocative interpretation, Rapa Nui Journal, 17, 119–122, 2003.

Dee, D., Uppala, S., Simmons, A., Berrisford, P., Poli, P., Kobayashi, S., Andrae, U., Balmaseda, M., Balsamo, G., Bauer, P., et al.: The ERA-Interim reanalysis: Configuration and performance of the data assimilation system, Quarterly Journal of the Royal Meteorological Society, 137, 553–597, 2011.

Direccion Meteorologica de Chile: Climatologia, http://164.77.222.61/climatologia/, online; accessed 09-February-2016.

Doms, G. and Baldauf, M.: A Description of the Nonhydrostatic Regional COSMO-Model Part I: Dynamics and Numerics, 2015.

Doms, G. and Schättler, U.: The nonhydrostatic limited-area model LM (Lokal-Modell) of DWD, Part I: Scientific documentation, Deutscher Wetterdienst (DWD), 1999.

Flenley, J. R. and King, S. M.: Late quaternary pollen records from Easter Island, 1984.

Flenley, J. R., King, A. S. M., Jackson, J., Chew, C., Teller, J., and Prentice, M.: The Late Quaternary vegetational and climatic history of Easter Island, Journal of Quaternary Science, 6, 85–115, 1991.

Gossen, C. L.: Deforestation, Drought and Humans: New Discoveries of the Late Quaternary Paleoenvironment of Rapa Nui (Easter Island), Ph.D. thesis, Portland State University, 2011.

Hunt, T. L. and Lipo, C. P.: Late colonization of Easter Island, Science, 311, 1603–1606, 2006.

Hunter-Anderson, R. L.: Human vs. climatic impacts at Rapa Nui: Did the people really cut down all those trees?, Easter Island in Pacific Context, 1998.

Junk, C. and Claussen, M.: Simulated climate variability in the region of Rapa Nui during the last millennium, Climate of the Past, 7, 579–586,

Kolb, P. F. and Robberecht, R.: High temperature and drought stress effects on survival of Pinus ponderosa seedlings, Tree Physiology, 16, 665–672, 1996.

Mann, D., Chase, J., Edwards, J., Beck, W., Reanier, R., and Mass, M.: Prehistoric destruction of the primeval soils and vegetation of Rapa Nui (Isla de Pascua, Easter Island), in: Easter Island, pp. 133–153, Springer, 2003.

Mann, D., Edwards, J., Chase, J., Beck, W., Reanier, R., Mass, M., Finney, B., and Loret, J.: Drought, vegetation change, and human history on Rapa Nui (Isla de Pascua, Easter Island), Quaternary Research, 69, 16–28, 2008.

Martinsson-Wallin, H.: Archaeological excavation at Vinapu (Rapa Nui), Rapa Nui Journal, 18, 7–9, 2004.

Martinsson-Wallin, H. and Crockford, S. J.: Early settlement of Rapa Nui (Easter Island), Asian Perspectives, pp. 244–278, 2001.

Mc Call, G.: Little Ice Age: Some proposals for Polynesia and Rapanui (Easter Island), Journal de la Société des Océanistes, 98, 99–104, 1994.

Mieth, A. and Bork, H.-R.: Humans, climate or introduced rats–which is to blame for the woodland destruction on prehistoric Rapa Nui (Easter Island)?, Journal of Archaeological Science, 37, 417–426, 2010.

Mieth, A., Bork, H.-R., and Feeser, I.: Prehistoric and recent land use effects on Poike peninsula, Easter Island (Rapa Nui), Rapa Nui Journal, 16, 89–95, 2002.

Orliac, C.: The woody vegetation of Easter Island between the early 14th and the mid-17th centuries AD, Easter Island archaeology: research on early Rapanui culture, pp. 211–220, 2000.

Clim. Past Discuss., doi:10.5194/cp-2016-68, 2016
Manuscript under review for journal Clim. Past
Published: 27 July 2016
© Author(s) 2016. CC-BY 3.0 License.

Orliac, C. and Orliac, M.: The disappearance of Easter Island's forest: overexploitation or climatic catastrophe, in: Easter Island in Pacific Context: South Seas Symposium. Proceedings of the Fourth International Conference on Easter Island and East Polynesia. Easter Island Foundation, Los Osos, pp. 129–134, 1998.

Rockel, B., Will, A., and Hense, A.: The regional climate model COSMO-CLM (CCLM), Meteorologische Zeitschrift, 17, 347–348, 2008.

Schrodin, R. and Heise, E.: The multi-layer version of the soil model TERRA_LM. Consortium for Small-Scale Modelling (COSMO), Tech. rep., Technical Report 2, 17 pp. http://www. cosmo-model. org, 2001.

Will, R. E., Wilson, S. M., Zou, C. B., and Hennessey, T. C.: Increased vapor pressure deficit due to higher temperature leads to greater transpiration and faster mortality during drought for tree seedlings common to the forest–grassland ecotone, New Phytologist, 200, 366–374, 2013.

Wilmshurst, J. M., Hunt, T. L., Lipo, C. P., and Anderson, A. J.: High-precision radiocarbon dating shows recent and rapid initial human colonization of East Polynesia, Proceedings of the National Academy of Sciences, 108, 1815–1820, 2011.

Clim. Past Discuss., doi:10.5194/cp-2016-68, 2016
Manuscript under review for journal Clim. Past
Published: 27 July 2016
© Author(s) 2016. CC-BY 3.0 License.

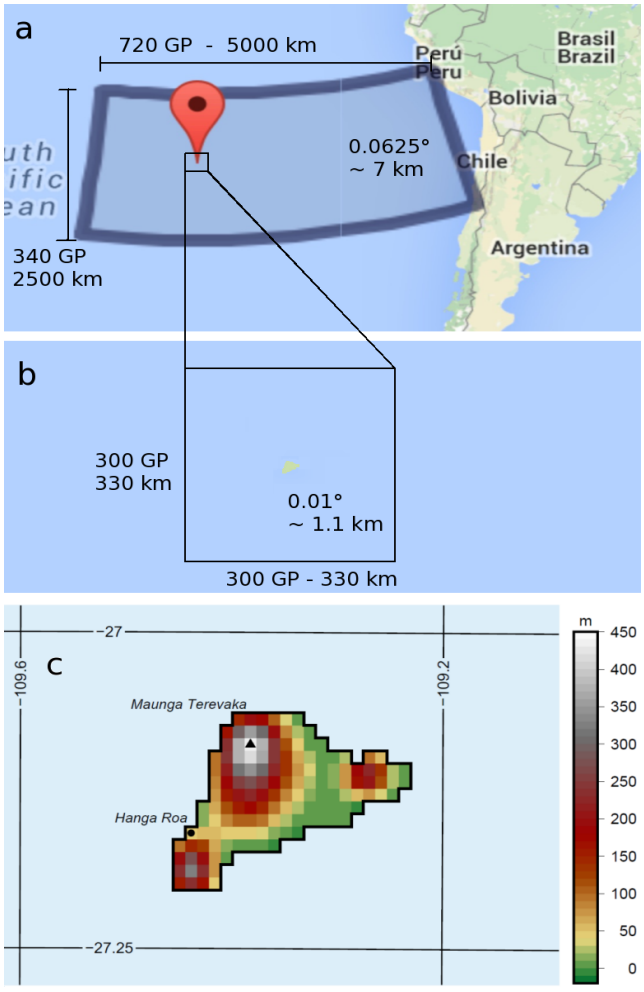

Figure 1. Model domain of coarse and fine simulation and land sea mask and topography of fine run. **a**) Dimension of the model domain of the preceding 7 km simulation which is driven by ECMWF analysis data at 0.25° resolution. **b**) Dimension of the final high resolution 1 km simulation which is driven by the output of the 7 km simulation. **c**) Land sea mask and topography in our high resolution simulations.

Clim. Past Discuss., doi:10.5194/cp-2016-68, 2016
Manuscript under review for journal Clim. Past
Published: 27 July 2016
© Author(s) 2016. CC-BY 3.0 License.

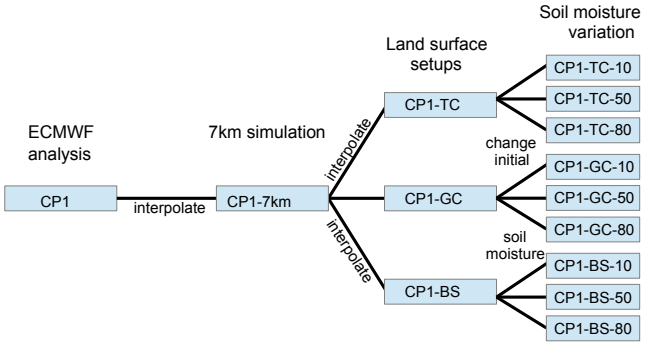

Figure 2. Scheme of nesting procedure and experiment setup. This is conducted for 14 synoptic case studies in total. Sometimes there are only 10% and 80% soil moisture experiments.

Clim. Past Discuss., doi:10.5194/cp-2016-68, 2016
Manuscript under review for journal Clim. Past
Published: 27 July 2016
© Author(s) 2016. CC-BY 3.0 License.

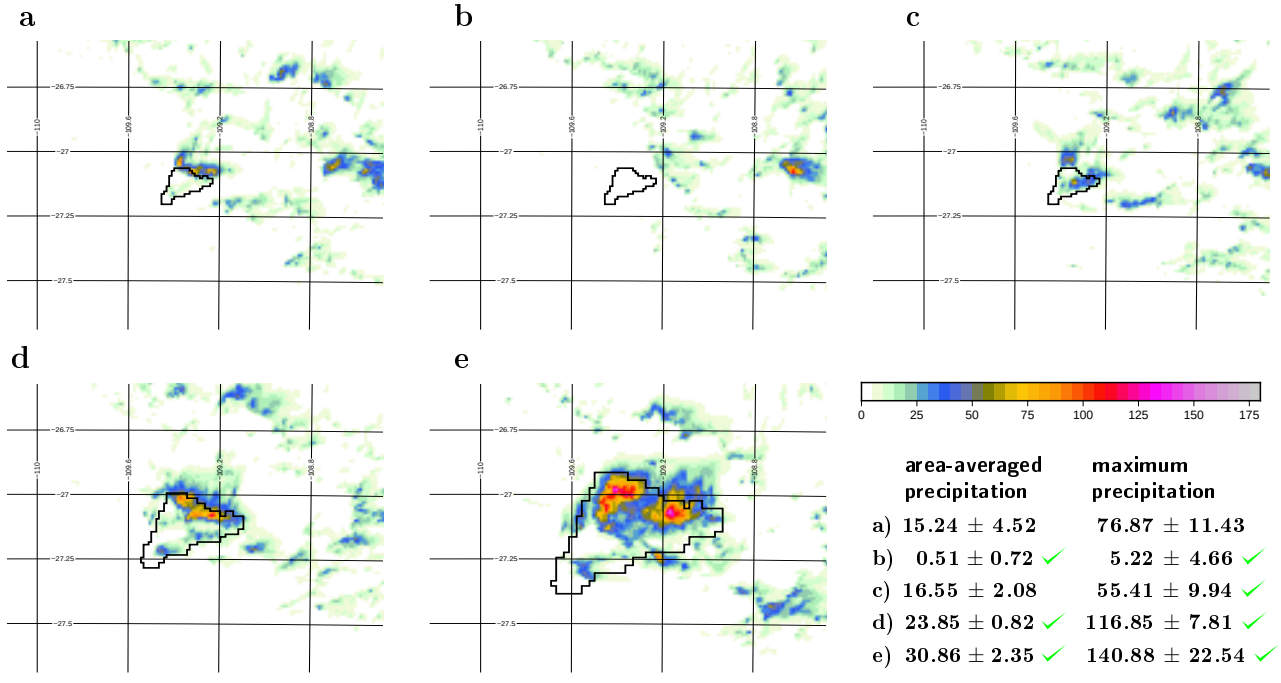

Figure 3. Precipitation sensitivity experiment for the synoptically undisturbed convective simulation CP1 with normal-sized/no/flat/enlarged island. 96-hour precipitation sum [mm] for simulation CP1: **a**) normal-sized island, **b**) no island, **c**) flat island, **d**) island enlarged by factor 4, **e**) island enlarged by factor 10. For each simulation ensemble member No. 1 is depicted. Mean and maximum values at the bottom right corner represent the 5-member ensemble mean of the island's spatial mean and island maximum. Checks indicate statistical significance of difference to normal-sized island simulation (t-test at 5% level)

Clim. Past Discuss., doi:10.5194/cp-2016-68, 2016
Manuscript under review for journal Clim. Past
Published: 27 July 2016
© Author(s) 2016. CC-BY 3.0 License.

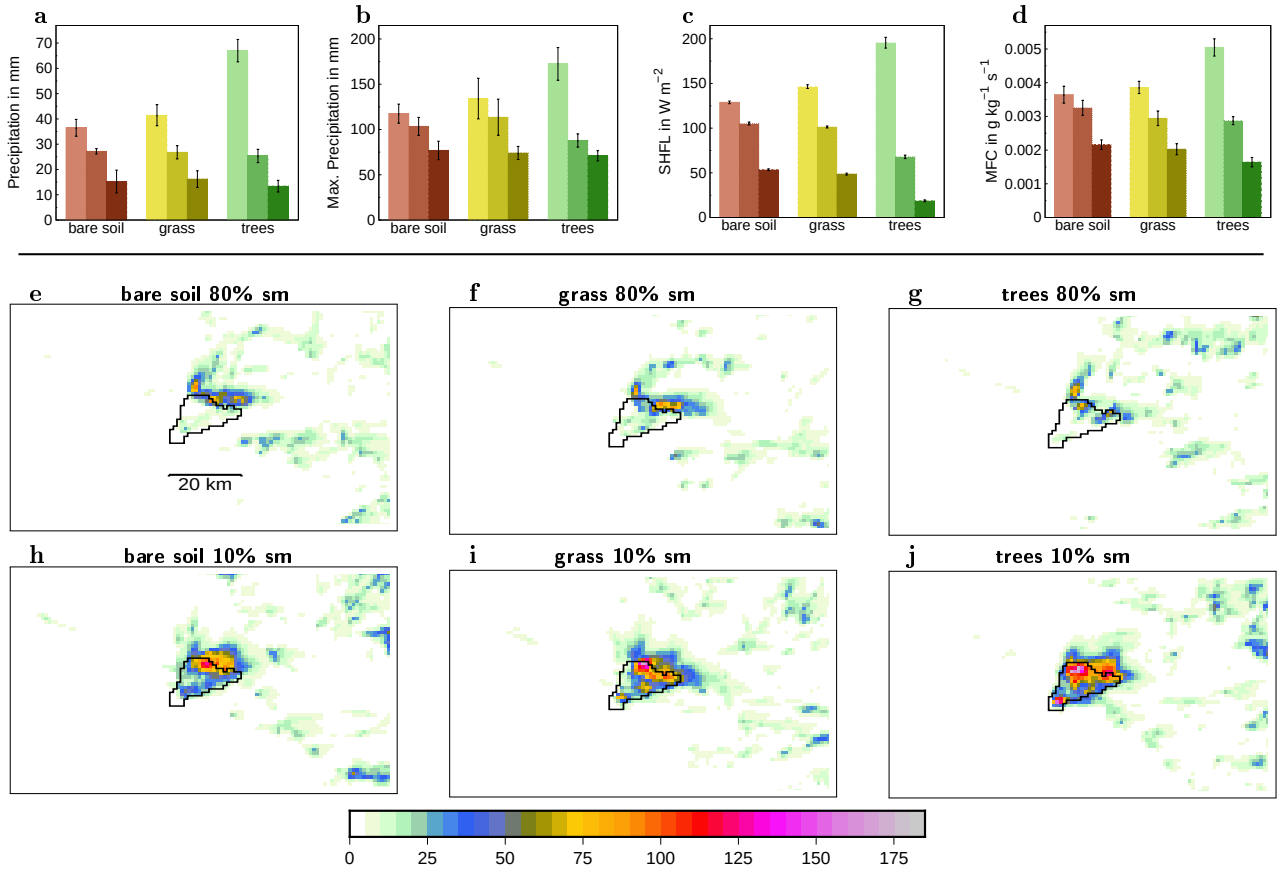

Figure 4. Precipitation, sensible heat flux and boundary layer moisture flux convergence for each land surface and soil moisture setting for the undisturbed convection case CP1 in December 2004. **a-d**) Easter Island spatial mean of: the 4-day accumulated precipitation (**a**), spatial maximum of the 4-day accumulated precipitation (**b**) the 4-day average of forenoon (0900LT-1200LT) sensible heat flux **(c)**, the 4-day average of afternoon (1200LT-1700LT) boundary layer moisture flux convergence (**d**). The lightest bars represent the low soil moisture case (10%), the darkest the high soil moisture case (80%), in-between the medium soil moisture case (50%). Error bars denote the standard deviation of the 5-member ensemble. (**e-j**) Spatial distribution of 4-day accumulated precipitation [mm] for 80% (**e-g**) and 10% initial soil moisture (**h-j**) . Shown are the results from one particular ensemble member.

Clim. Past Discuss., doi:10.5194/cp-2016-68, 2016
Manuscript under review for journal Clim. Past
Published: 27 July 2016
© Author(s) 2016. CC-BY 3.0 License.

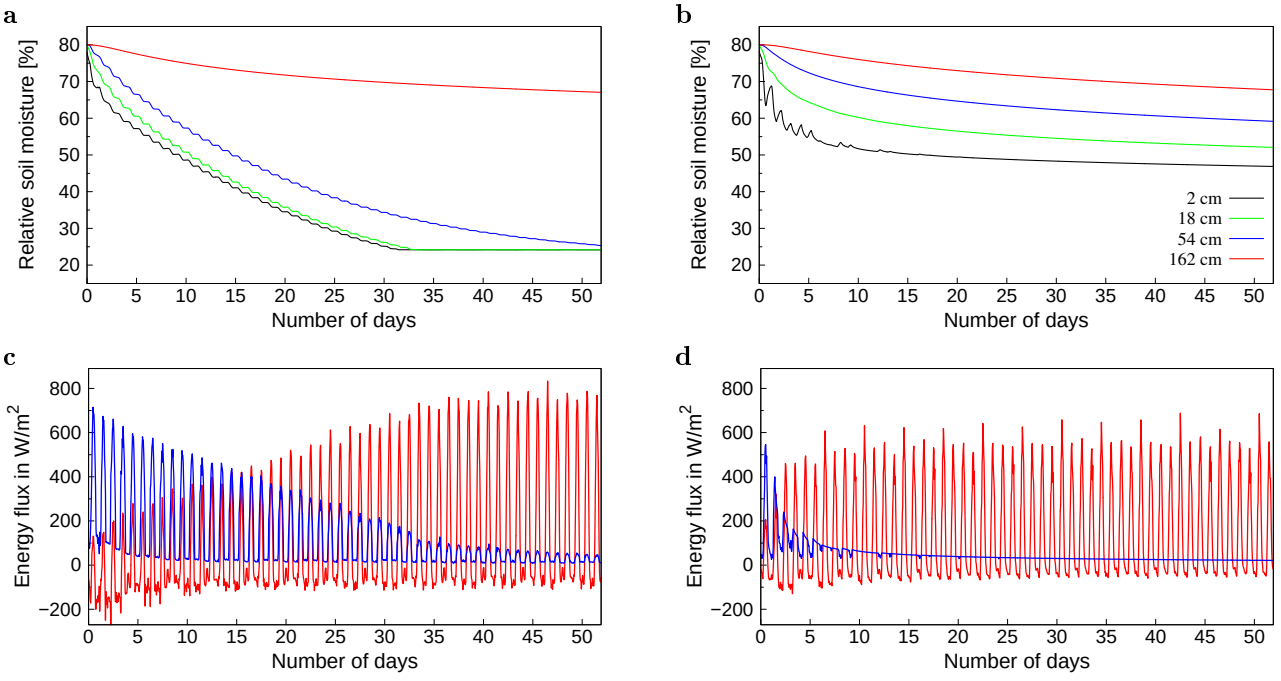

Figure 5. 52 day long soil drying experiment for tree-covered and bare soil island. **a-b**) Time series of soil moisture relative to pore volume [%] for four different soil depths for the tree-covered island (**a**) and the bare soil island (**b**). **c-d**) Corresponding time series of sensible (red lines) and latent heat fluxes (blue lines) [W/m^2] for the tree-covered island (**c**) and the bare soil island (**d**).

Clim. Past Discuss., doi:10.5194/cp-2016-68, 2016
Manuscript under review for journal Clim. Past
Published: 27 July 2016
© Author(s) 2016. CC-BY 3.0 License.

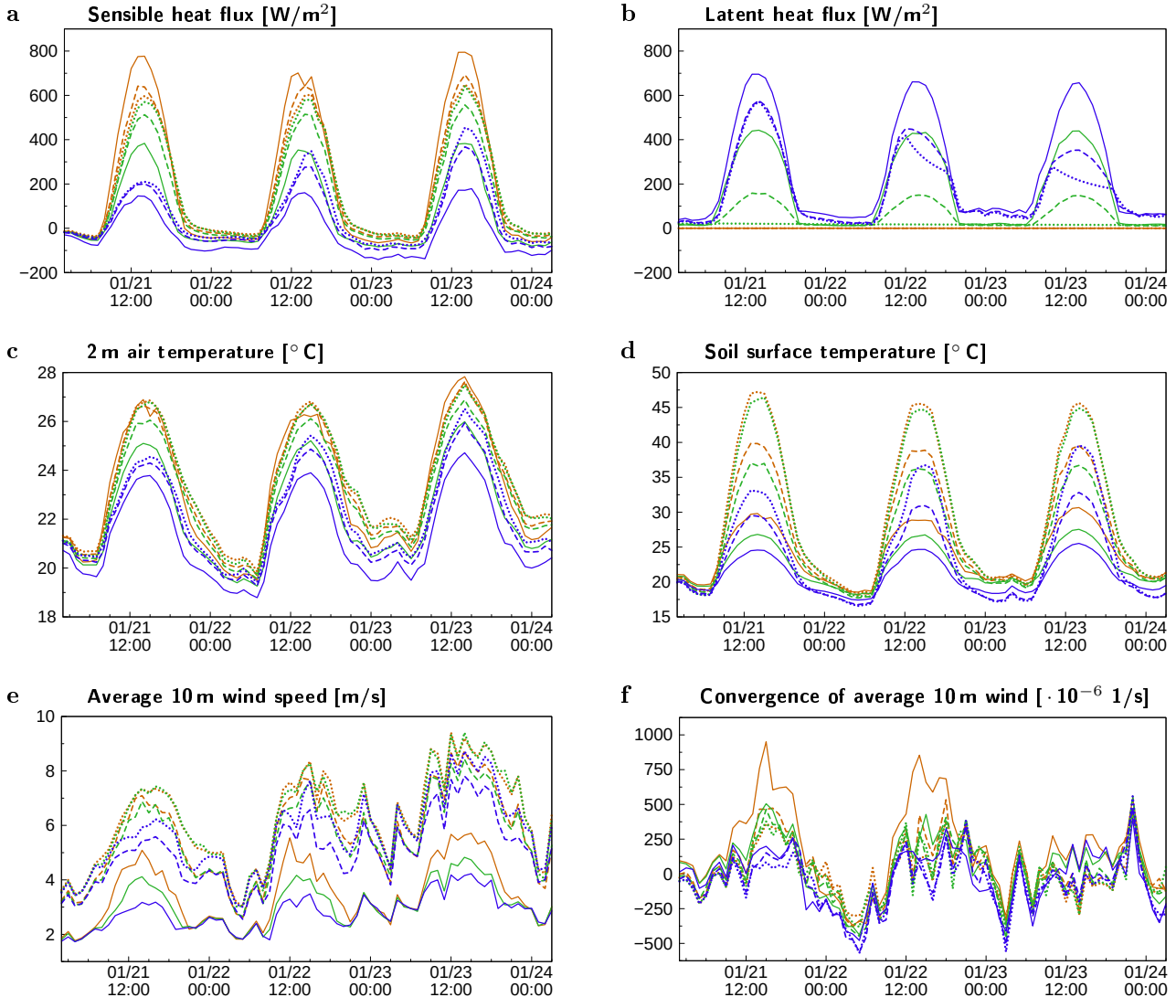

Figure 6. Area-averaged turbulent heat fluxes, soil and near surface air temperatures, wind speeds and convergence for the high-insolation case study CSC1 in January 2011. For all figures, the solid lines depict the tree-covered, the dashed line the grass-covered and the dotted line the bare soil island. Blue colours represent the 80% soil moisture setting, green 50% and ochre 10%.

Clim. Past Discuss., doi:10.5194/cp-2016-68, 2016
Manuscript under review for journal Clim. Past
Published: 27 July 2016
© Author(s) 2016. CC-BY 3.0 License.

Climate of the Past Discussions
Open Access
EGU

Table 1. Relative change of area-averaged Easter Island precipitation due to a complete deforestation (bare soil minus tree-covered) for the four low wind convective cases CP1-CP4 depending on initial soil moisture. Changes that cannot be considered statistically significant by student t-test are greyed out. The precipitation differences in the dry-soil cases are clearly statistically significant. The highest p-value of 0.91 % occurs in CP4 which is still well below the common threshold of 5%. Precipitation changes of CP2 with 50% and 80% soil moisture are omitted due to the too low amounts of rain.

	10% soil moist.	50% soil moist.	80% soil moist.
CP1	$-41.6 \pm 4.9\%$	$+7.2 \pm 11.2\%$	$+13.7 \pm 37.9\%$
CP2	$-73.7 \pm 17.9\%$	-	-
CP3	$-40.3 \pm 5.1\%$	$+11.7 \pm 7.8\%$	$+20.5 \pm 14.7\%$
CP4	$-29.4 \pm 17.2\%$	$+13.7 \pm 34.3\%$	$-3.6 \pm 42.4\%$

Clim. Past Discuss., doi:10.5194/cp-2016-68, 2016
Manuscript under review for journal Clim. Past
Published: 27 July 2016
© Author(s) 2016. CC-BY 3.0 License.

Climate of the Past Discussions
Open Access
EGU

Table 2. Near-surface climate differences between humid forested island (TC-80) and less humid bare soil Easter Island (BS-50) in clear-sky conditions case studies CSC1-CSC3. As a reference, the mean short-wave radiation (from BS-50), the synoptic scale mean wind speed in Easter Island region, the sea surface temperature and the total cloud cover (from BS-50) are given. Compared are the changes in area-averaged temperature maximum (2 m air and soil surface), absolute change in area-averaged relative humidity minimum, and the relative wind speed changes due to deforestation (BS-50 minus TC-80), p.p. stands for percentage points

	CSC1	CSC2	CSC3
Midday net SW$\downarrow$ (BS-50) [W/m^2]	918	787	418
Synop. scale $v_{10\mathrm{m}}$ [m/s]	6.3	3.9	6.1
SST [$^\circ$C]	24.5	21.3	21.2
total cloud cover (BS-50) [%]	20	30	61
$\Delta T_{2\mathrm{m}}^{\mathrm{max}}$ (BS-50 $-$ TC-80) [K]	+2.8	+2.6	+1.8
$\Delta T_{\mathrm{S}}^{\mathrm{max}}$ (BS-50 $-$ TC-80) [K]	+20.9	+22.4	+10.7
$\Delta RH_{2\mathrm{m}}^{\mathrm{min}}$ (BS-50 $-$ TC-80) [p.p.]	-18.5	-25.8	-24.5
$\Delta\, v_{10\mathrm{m}}$ (BS-50 $-$ TC-80) [%]	+82.0	+106.0	+94.3